

## **Border Fertigation : Field Experiments and Simple Model**

**E. Playán<sup>1</sup> and J. M. Faci<sup>2</sup>**

<sup>1</sup> (O) Dept. Genetics and Plant Production,  
Lab. for Agronomy and the Environment (DGA-CSIC).  
Estación Experimental de Aula Dei, CSIC  
Apdo. 202. 50080 Zaragoza, Spain  
Fax : + 34 76 575620  
Email : playan@eead.csic.es

<sup>2</sup> Dept. Soils and Irrigation,  
Lab. for Agronomy and the Environment (DGA-CSIC).  
Servicio de Investigación Agroalimentaria, DGA  
Apdo. 727. 50080 Zaragoza, Spain

### **Abstract**

Fertilizers are commonly dissolved in border irrigation water. However, there are no available procedures for proper design and management of surface fertigation. A series of experiments was conducted to determine the uniformity of fertilizer application under varying inflow discharges and fertilizer application times in blocked-end borders. Results from the fertigation evaluations showed that the fertilizer distribution uniformity of the low half (DULH) ranged from 2.9 to 51.6% while water DULH ranged from 63.5 to 96.9%. A simplified border fertigation model based on one-dimensional convection was formulated and applied to the simulation of the experiments. The model was able to explain 43.8% of the variability in the fertilizer DULH. Application of the model to selected case studies revealed that short duration applications, such as those resulting from instantaneous release of fertilizer into the irrigation stream, often produce low uniformities. This is particularly true for early applications in blocked-end borders and for early and late applications in level-basins. In both irrigation systems, application of fertilizer at a constant rate during the entire irrigation event is frequently the best solution. In the

presence of runoff, the model can be used to find a compromise between fertilizer application uniformity and runoff losses. Finally, if large deep percolation losses are expected, the model can identify uniform fertigation options based on late applications of fertilizer.

## **Introduction**

Fertilization is one of the key factors in obtaining profits from agricultural crops. In many cases, use of the customary fertilizer distribution machinery is hindered by inherent conditions of the crop. Such is the case of corn, a crop with high nitrogen requirements, long growth cycle and tall canopy. In semiarid environments, corn is irrigated frequently, and a significant part of the applied nitrogen fertilizer is leached by deep percolation. Under these conditions the best fertilizer management options are based on small and frequent nitrogen applications. Unfortunately, tractor operations in corn are not possible after just a few weeks from sowing, and farmers usually resort to fertigation.

Viets *et al.* (1967) reported that, at the time, about 5% of the nitrogen fertilizer sold in California was applied in irrigation water. Threadgill (1985) conducted a chemigation survey in the United States and found that chemigation was used at least once a year on 4.3 million ha. While 61% of the microirrigation systems and 43% of the sprinkler systems used chemigation, only 3.5% of the surface irrigation systems utilized this technique. Threadgill *et al.* (1990) attributed this to the typical low uniformity of surface irrigation systems and to the fertilizer losses due to runoff. Recently, Hanson *et al.* (1995) reported the results of a study based on 959 field evaluations of irrigation systems in California. Remarkably, they found that the uniformity of border and furrow irrigation was relatively higher than that of all other systems. In the light of these findings, further study of surface fertigation seems to be of interest.

The first attempts to perform surface fertigation used solid fertilizers. A practice still in use in some areas is instantaneous release of fertilizer in the irrigation

stream. In this case the fertilizer application uniformity will usually be poor. If the irrigation uniformity is low, a pulsed fertilizer application starting at the right time can result in a good fertilizer uniformity. Lately, use of nitrogen solutions has resulted in fertilizer applications lasting as long as the irrigation event (mixing fertilizer and fresh water at a constant rate). In this case, the fertilizer application uniformity will be the same as that corresponding to the irrigation water (Viets *et al.*, 1967). Unfortunately this is not the end of the problem, for three reasons. First, irrigation uniformity can be low, resulting in a poor fertilizer management. Second, many irrigation systems are operated under high runoff losses, which result in dumping of large amounts of fertilizers directly to the runoff stream. Finally, even if the irrigation event is uniform, the efficiency can be low due to excessive deep percolation losses. In this case, the fertilizer will leach out of the root zone and become both a loss and an environmental hazard. Environmental concerns related to fertilization practices are gaining importance, as new cases of fertilizer-related eutrophication of water courses and degradation of aquifers are reported constantly.

The physico-chemical interaction between the fertilizer and the soil porous medium makes it difficult to estimate fertilizer deep percolation losses. This is the reason why in this work the adequacy of fertilizer application is expressed in terms of uniformity and runoff losses. Recent developments in overland water flow (Katopodes, 1994) and soil solute tracing under both border and furrow irrigation (Jaynes *et al.*, 1992 ; Izadi *et al.*, 1996) announce the future development of integrated fertigation models.

In this work we report the results of ten border fertigation evaluations. These experiments were designed to explore the performance of fertigation under a restricted set of operating conditions. A simplified model of border fertigation is presented to assist in decision making as applied to the timing of fertilizer application for a given irrigation event. The results of the experiments are used to assess the predictive capability of the model in terms of fertilizer application and distribution uniformity. The model was finally used to explore the suitability of border fertigation under a wide set of operating conditions.

## **Materials and Methods**

### **Field experiments**

Ten field experiments were performed to evaluate border irrigation performance and the distribution of fertilizer. The field was laser leveled to a uniform longitudinal slope of 0.001 %. The border strips had no provision for runoff. Irrigation was cut-off before the end of the advance phase to diminish the chances of waterlogging at the downstream end. All irrigation evaluations were performed following the procedures reported by Merriam and Keller (1978), except when otherwise stated.

A neutrally buoyant solute (ammonium nitrate or potassium bromide) was uniformly added to the irrigation water at the upstream end of the border. Gated pipe was used to deliver water to the strips. The turbulence resulting from the jets dissolved and homogenized the solute in the irrigation water. The solute concentration resulted in an electrical conductivity (EC) that could be distinguished from that of fresh irrigation water with the help of a field EC meter. EC of the fertilized water reached peak values of  $16 \text{ dSm}^{-1}$ , while the EC of fresh water was  $1.6 \text{ dSm}^{-1}$ .

After application of the solute, water samples were collected at a number of stations located along the borders. At each station, water sampling started as soon as the conductivity meter detected the approaching solute plume. Sampling frequency was as high as one sample per minute when the conductivity meter revealed transients in solute concentration. Sampling stopped at a given station when the EC dropped to the value characteristic of fresh irrigation water. Water samples were analyzed using ionic chromatography (Tabatabai and Dick, 1983).

Infiltration was characterized using the well-known Kostiaikov-Lewis equation :

$$Z = k\tau^a + f_0\tau \quad [1]$$

where  $Z$  is the infiltrated depth (m),  $\tau$  is the opportunity time (min),  $k$  is an empirical coefficient ( $\text{m min}^{-a}$ ),  $a$  is a dimensionless empirical exponent, and  $f_0$  is an empirical coefficient ( $\text{m min}^{-1}$ ). At each water sampling station the solute application was estimated using the overland water concentration and the infiltration equation. The mass of solute infiltrated between two consecutive water samplings can be estimated as the difference between the corresponding infiltrated depths times the average concentration of the overland water ( $C$ ,  $\text{g m}^{-3}$ ). If the total number of samples is  $m$ , the solute application ( $A$ ,  $\text{g m}^{-2}$ ) can be estimated as :

$$A = \sum_{i=1}^{i=m-1} (Z_{i+1} - Z_i) \frac{(C_{i+1} + C_i)}{2} \quad [2]$$

We performed one field experiment using bromide and nine field experiments using nitrate. The peculiarities of each type of experiments are detailed in the following paragraphs.

**Bromide experiment.** The purpose of this fertigation evaluation was to provide a means to assess the validity of the estimations and model predictions of fertilizer application. For this reason, we used KBr, a conservative mobile tracer widely used in this sort of studies (Jaynes *et al.*, 1992 ; Izadi *et al.*, 1996). Previous soil analyses confirmed that  $\text{Br}^-$  was not present in the soils of the experimental field. A fertigation evaluation was performed on a blocked-end border with dimensions 255 m and 3.84 m. The unit discharge was  $4.53 \text{ l s}^{-1} \text{ m}^{-1}$ , and the irrigation time was 44 min. The field had just been ripped and rolled. According to the results of previous trials, a value of 0.03 was selected for Manning  $n$ . A total amount of 23.22 kg of potassium bromide (48.30%  $\text{Br}^-$ ) was evenly applied during 7 min (between times 18 and 25 min).

Stations were marked at 25 m intervals to ease the observation of the times of advance and recession. Soil samples were collected at six alternate stations (separated 50 m) to a depth of 1.2 m in 0.3 m increments to determine bromide content in soil using ionic chromatography (Nieto and Frankenberger, 1985). Two soil samples were collected at each station and soil layer. At the remaining five

stations, water samples were collected and analyzed for  $\text{Br}^-$ , water recharge was determined gravimetrically and infiltration was measured using cylinder infiltrometers. Determinations of infiltration and water recharge were separated across the border in order to avoid interferences between the experimental procedures.

The observations of infiltration and opportunity time at each cylinder were used to estimate the local parameters of equation [1] using regression analysis. The spatially averaged infiltration parameters of the border were obtained by regression of a data set containing the observations of all five cylinders. Local and spatially averaged parameters were adjusted using the procedure described by Merriam and Keller (1978). This procedure is based on the adjustment of the parameter  $k$  of equation [1] to ensure that the applied irrigation volume is infiltrated at the average observed opportunity time. Both sets of infiltration parameters were alternatively used to estimate the bromide application, in an attempt to establish the relevance of the spatial variability of infiltration.

**Nitrate experiments.** The purpose of these experiments was to further explore the predictive capability of the proposed fertigation model in terms of fertilizer application and distribution uniformity. For this matter, we performed fertigation evaluations in nine blocked-end border configurations made up of combinations of three inflow discharges and three fertilizer application times. The application times were dictated by the course of the advance process. Fertilizer application started at 0%, 33% and 50% of advance for the A1, A2 and A3 cases, respectively. A fertilizer application time of 5 min was used in all experiments. The inflow discharges were labeled Q1, Q2 and Q3, and their average values were 3.36, 4.94, and 7.82  $\text{l s}^{-1} \text{m}^{-1}$ , respectively.

In each evaluation, 100 kg of nitrogen fertilizer based on ammonium nitrate (with a 53.19 % of  $\text{NO}_3^-$ ) were applied. Due to the initial content of  $\text{NO}_3^-$  in the soil as well as to its physico-chemical transformations in the soil-root environment, no  $\text{NO}_3^-$  soil analyses were performed. Table 1 presents the unit discharge, border width, cut-off

time, starting time ( $t_s$ ) and ending time ( $t_e$ ) of fertilizer application. A crop of corn was well established in the borders by the time of the experiments. According to previous experiments in the same field, a value of 0.04 was chosen for Manning  $n$ .

The borders were 280 m long and between 2.90 and 3.55 m wide (Table 1). The times of advance and recession were recorded at eight stations set at 40 m intervals. Water samples were collected at the same stations and analyzed for  $\text{NO}_3^-$ . The spatially averaged parameters of the Kostiakov-Lewis infiltration equation were estimated for each irrigation event by best fit to the observed advance-recession curve. A hydrodynamic surface irrigation model (Walker, 1993) was used for this purpose in an iterative fashion.

### **A simplified surface fertigation model**

The transport of neutrally buoyant conservative substances in open channel flows was described in detail by Cunge *et al.* (1980). The solute transport process occurring in surface fertigation can be considered as the result of hydrodynamic dispersion. This process is the interaction between differential convection and turbulent diffusion. In one spatial dimension, the longitudinal dispersion of a fully mixed tracer follows a Fickian diffusion law, of the form :

$$\frac{\partial}{\partial t}(hC) + \frac{\partial}{\partial x}(hvC) = \frac{\partial}{\partial x}\left(hK_x \frac{\partial C}{\partial x}\right) \quad [3]$$

where  $h$  is the flow depth,  $v$  is the vertically averaged flow velocity, and  $K_x$  is the longitudinal mixing coefficient.

Equation [3] can be numerically solved for  $C(x,t)$  once the flow depth and flow velocity fields are known, and proper initial and boundary conditions for  $C$  are devised. The output of a surface irrigation simulation model can be used as a source of  $h(x,t)$  and  $v(x,t)$  values, since the open channel flow and the transport processes can be solved in an uncoupled fashion. Problems in obtaining sensible results from equation [3] may stem from the need to estimate the additional parameter  $K_x$  and

from an inherent limitation of the equation: The Fickian approximation is only strictly valid at large distances from the injection point.

An additional limitation of the one-dimensional Fickian approach as applied to surface fertigation lies in the hypothesis behind the Saint Venant equations, particularly in the fact that they are vertically averaged. Katopodes (1994), aware of the limitations inherent to this approach as applied to the analysis of processes such as fertigation, developed a first attempt to model the vertical structure of flow velocity in an advancing front. His model was based on the solution of the turbulent Navier-Stokes equations using a finite element approach. The author suggested that further developed versions of his model (for the front region) could be combined with vertically averaged models (applied to the upstream region in combination with a velocity distribution pattern) to yield accurate descriptions of solute transport.

**Model description.** It is our opinion that for the current state of science, a simple model of surface fertigation can be of use, particularly since the topic of assessing surface fertigation uniformity has not been previously addressed *via* modeling. This simplified model will be based on neglecting the vertical velocity field and the process of turbulent diffusion. In this way, the flow section entering the domain at time  $t_s$  will permanently separate fresh and fertilized water in its movement downstream. The trajectory of a particle located in this section will determine the advance trajectory of the fertilizer.

The model is therefore based on the hypothesis that fresh and fertilized water do not mix during the overland phase of the irrigation event. The plume of fertilized water is convected downstream in a one-dimensional fashion, and the fertilizer infiltrates according to the local opportunity times. Under this assumption, the constant fertilizer concentration can be computed as :

$$C = \frac{MF}{QW(t_e - t_s)} \quad [4]$$

where  $MF$  is the total mass of fertilizer applied,  $Q$  is the unit discharge in the border and  $W$  is the border width. In the proposed model, the results of a hydrodynamic

surface irrigation model (Walker, 1993) are used to compute the fertilizer advance and recession trajectory. For this matter, estimates of  $h$  and  $v$  are required at the nodes of a regular  $(x, t)$  network. In all presented model runs,  $\Delta x$  was taken as 1 m and  $\Delta t$  as 1 min.

A schematic representation of a surface fertigation event is presented in Fig. 1. Between times  $t$  and  $t+\Delta t$  the fertilized plume (represented by the shadowed area in the figure) travels downstream. At time  $t$  the advancing front of the fertilizer was located at a distance  $XA_t$ , while the recession front was located at  $XR_t$ . At time  $t+\Delta t$  the plume is delimited by distances  $XA_{t+\Delta t}$  and  $XR_{t+\Delta t}$ . The location of the fertilizer advancing front at time  $t+\Delta t$  can be computed as:

$$XA_{t+\Delta t} = XA_t + \frac{v_t + v_{t+\Delta t}}{2} \Delta t \quad [5]$$

A mass conservation equation between the considered time steps can be written in the following terms:

$$M_{t+\Delta t} = M_t + MF_t^{t+\Delta t} - SRO_t^{t+\Delta t} - I_t^{t+\Delta t} \quad [6]$$

where  $M$  is the total overland mass of fertilizer,  $SRO$  is the mass of fertilizer lost by surface runoff, and  $I$  is the mass of infiltrated fertilizer. Variables with a time subindex express the value of the variable at that specific time. Variables with a time subindex and a time superindex express the fertilizer added to or subtracted from the total overland mass between both times by fertigation, runoff or infiltration. The following equations express the procedure used in the model to advance the solution by one time step.

As expressed in Fig. 1,  $\Delta t$  is divided in two subintervals. In the first subinterval (between  $t$  and  $t+\frac{\Delta t}{2}$ ) the dependent variables  $h$  and  $v$  take the values corresponding to the time step  $t$ . Correspondingly, the values for  $h$  and  $v$  in the second subinterval correspond to time  $t+\Delta t$ . Mass transfers due to fertigation, runoff and infiltration can be broken down in the following way:

$$M_{t+\Delta t} = M_t + \left( MF_t^{t+\frac{\Delta t}{2}} + MF_{t+\frac{\Delta t}{2}}^{t+\Delta t} \right) - \left( SRO_t^{t+\frac{\Delta t}{2}} + SRO_{t+\frac{\Delta t}{2}}^{t+\Delta t} \right) - \left( I_t^{t+\frac{\Delta t}{2}} + I_{t+\frac{\Delta t}{2}}^{t+\Delta t} \right) \quad [7]$$

The overland mass of fertilizer at the beginning of the time step ( $M_t$ ) is known, and it takes a zero value prior to any fertilizer application. The mass of fertilizer applied in each subinterval is equally known since fertilizer application is part of the definition of the problem.

If  $XA$  coincides with the downstream boundary condition ( $DSBC$ ) and runoff is permitted, fertilizer runoff will occur, and  $SRO$  will take a nonzero value that can be computed using equations [8] and [9].

$$SRO_t^{t+\frac{\Delta t}{2}} = CW h_{(DSBC,t)} v_{(DSBC,t)} \frac{\Delta t}{2} \quad [8]$$

$$SRO_{t+\frac{\Delta t}{2}}^{t+\Delta t} = CW h_{(DSBC,t+\Delta t)} v_{(DSBC,t+\Delta t)} \frac{\Delta t}{2} \quad [9]$$

The mass of fertilizer infiltrated during the first subinterval can be computed as:

$$I_t^{t+\frac{\Delta t}{2}} = CW \sum_{x=XR_t}^{x=XA_t} \left( Z_{(x,t+\frac{\Delta t}{2})} - Z_{(x,t)} \right) \Delta x \quad [10]$$

All the known terms in equation [7] can be grouped in a constant called  $\Omega$ .

Therefore,

$$M_{t+\Delta t} = \Omega - I_{t+\frac{\Delta t}{2}}^{t+\Delta t} \quad [11]$$

The two unknown terms are the final mass of overland fertilizer and the mass of fertilizer infiltrated during the second subinterval. Both terms can be expanded in the following way:

$$CW \sum_{x=XR_{t+\Delta t}}^{x=XA_{t+\Delta t}} h_{(x,t+\Delta t)} \Delta x = \Omega - CW \sum_{x=XR_{t+\Delta t}}^{x=XA_{t+\Delta t}} \left( Z_{(x,t+\Delta t)} - Z_{(x,t+\frac{\Delta t}{2})} \right) \Delta x \quad [12]$$

The only unknown in equation [12] is the location of the recession front of the fertilizer plume at time  $t+\Delta t$  ( $XR_{t+\Delta t}$ ). The proposed model determines this variable iteratively, proceeding backwards one node at a time from  $XA_{t+\Delta t}$  until equation [12] is satisfied.

Simulation comes to an end when the mass of applied fertilizer is consumed by infiltration and runoff. At this time, the mass of infiltrated fertilizer can be computed for each node using equation [2], further simplified by the fact that  $C$  is

supposed to be time and space invariable. Performance indexes can be computed following the uniformity coefficients described for infiltrated irrigation depth. We used the distribution uniformities of the low quarter and the low half (DULQ and DULH, respectively) as described by Merriam and Keller (1978).

**Model application.** The proposed model was first applied to the simulation of the field experiments in order to assess its predictive capability. In a second step, the model was used to explore the merit and limitations of surface fertigation, particularly the timing and length of the fertilizer application period. The first case study involved the simulation of experiment A1Q1 with all feasible combinations of  $t_s$  and  $t_e$  taken at 10 min steps. The remaining case studies involve modifications of the same experiment.

Case A1Q1-LB reproduces a level-basin irrigation event: the field slope was set to zero and the cut-off time was extended to 150 min to ensure complete advance. The third numerical experiment (called A1Q1-SRO) explores the case of free draining borders, where the maximization of the fertilizer distribution uniformity must be combined with the minimization of fertilizer runoff losses. The cut-off time was extended from 70 to 110 min and the downstream boundary condition was modified to permit runoff.

Finally, case study A1Q1-DP was devised to assess surface fertigation practices in the presence of low water DULH or large deep percolation losses. For this matter, the infiltration parameters in A1Q1 were replaced by those characterizing the 1.0 family of infiltration curves as defined by the Natural Resources Conservation Service and adapted to the Kostiakov-Lewis infiltration equation (Walker, 1989). The cut-off time was adjusted accordingly, to a value of 500 min.

## **Results and Discussion**

### **Bromide experiment**

The results of the adjusted infiltration measurements are presented in Table 2. The coefficients of determination are high for the local ring infiltrometer regressions, while the value corresponding to the spatially averaged infiltration regression (75.5%) reflects the differences between the infiltrometer rings. Fig. 2 presents the irrigation water advance and recession curves as observed and predicted by the model. The simulated recession time at the downstream end of the border (not shown in the figure) was 543 min. Agreement between the advance observations and the hydrodynamic model is satisfactory except for the downstream end of the border. At this point, the slowing effect of cut-off on advance was more evident in the experiment than in the model. Small scale disturbances in land leveling could be partially responsible for this lack of agreement. In the recession phase, agreement is not so satisfactory. This is due in part to the poor prediction of the recession phase under blocked-end conditions. No field observations of recession are available beyond 175 m.

The predicted advance and recession trajectory of the tracer are presented in the same figure. In this experiment, the bromide opportunity time is very similar along the border, except for the downstream end. The differences in the resulting bromide application are mainly due to the local infiltration rates at the times of fertilizer advance and recession.

Fig. 3 presents the measurements and predictions of bromide concentration vs. opportunity time at five locations along the border. Hydrodynamic dispersion lowers the peak and broadens the base of the bromide concentration curve as it travels downstream. At 25 m the prediction of the peak concentration is accurate whereas, at longer times, the observed peak concentration is lower than predicted. In general, the model predicts a shorter than real fertilizer opportunity time. This is compensated by the higher, invariable fertilizer concentration. In coincidence with Fig. 2, as the fertilizer plume travels downstream, it reaches the stations earlier in the infiltration process, when the infiltration rate is higher. As a result, fertilizer application should increase with distance down the border. At a distance 225 m, the measured concentration indicates that the plume had already reached the advancing

front, while the model still predicted a short lag between water and fertilizer advance. The spatial variability of infiltration can also be a major source of differences between predicted and measured values of bromide concentration in irrigation water.

The resulting distribution of bromide application along the border is presented in Fig. 4. Measurements, estimations and predictions indicate a steadily growing bromide application with distance. At the downstream end of the border, model predictions indicate a steep rise in the bromide application, reaching a peak value of  $137 \text{ g m}^{-2}$ . This peak is signaled by a large value of the measured bromide application at a distance of 250 m. Agreement between the three sources of data is satisfactory. Measurements and observations accounted for 69% and 66% of the applied bromide mass, respectively. Our results indicate that the missing bromide was not lost by deep percolation. In fact, soil bromide decreased with depth at all stations from the upper layer (0-30 cm), and the bromide content beyond 60 cm was negligible. Therefore, we are inclined to think that at unsampled locations, presumably at the downstream end, the application was higher than the average, as suggested by the model and the measured soil bromide application at 250 m. A correlation study between predicted and measured bromide application indicated that  $r = 0.986$  ( $P < 0.001$ ). Correspondingly, the correlation coefficient between estimations and model predictions was 0.950 ( $P = 0.013$ ).

The five local infiltration equations were used to explore the relevance of the spatial variation of infiltration on the water and fertilizer application. To obtain estimations of water application, the spatially averaged and the five local infiltration equations were alternatively combined with the observed opportunity times. Use of local infiltration parameters improved the correlation coefficient between measured and estimated water application from an unrealistic -0.615 ( $P = 0.385$ ) to 0.982 ( $P = 0.018$ ). The same procedure was used to estimate the fertilizer application. In this case, however, the results were not as conclusive, since use of the local infiltration parameters reduced the correlation coefficient between estimations and model predictions from the reported 0.950 ( $P = 0.013$ ) to 0.902 ( $P = 0.036$ ). Due to the high

spatial variability of infiltration, we believe that a finer grid for infiltration measurement would have led to more conclusive results.

### **Nitrate experiments**

Table 3 presents the results of infiltration parameter estimation for the nine fertigation evaluations. Although the borders were located adjacent to each other, the spatially averaged infiltration parameters reveal important differences. Fig. 5 presents plots of estimated and predicted nitrate application against border length for each irrigation event. The eight estimations of fertilizer application per evaluation were used to estimate the total mass of applied nitrate. The average value indicates that 97.3% of the applied nitrate was accounted for by the estimation process. The corresponding standard deviation (among the nine evaluations) was 21.6%.

A first glance of Fig. 5 indicates that fertilizer application is strongly nonuniform. The uniformity parameters presented in Table 3 indicate that in the considered cases, water application was much more uniform than fertilizer application. Under very nonuniform conditions, DULH is better suited than DULQ. That is why we recommend use of DULH for the characterization of fertilizer uniformity in short duration surface fertigation events. Due to the simplified nature of the model, the predicted fertilizer DULH is consistently lower than estimated DULH (except for case A3Q1). The beneficial effect of differential convection and dispersion seems clearly reflected in evaluations A1Q3, A2Q2 and A3Q3. In the three cases the estimations of fertilizer application (computed from overland water nitrate concentration) fall well over model predictions. In A1Q3 and A2Q2 dispersion projected the fertilizer forward down the border, whereas in A3Q3 dispersion resulted in a sustained concentration of fertilizer behind the peak value. Considering the eight sampling stations per evaluation, the model is able to explain 29.3% ( $P < 0.001$ ) of the variance in the estimated application. When estimated and predicted DULH's are compared, the model can explain 43.8% ( $P = 0.052$ ) of the variance in the estimated uniformity (Fig. 6). Although the statistical significance of this last regression is weak, the proposed model shows promise to assist in the

analysis and management of surface fertigation. The model yields low, conservative predictions of fertilizer uniformity.

The fertigation evaluations in this experiment are subjected to two important sources of dissimilarities : the inter-border variability of infiltration and the adequacy of the time of cut-off. As a consequence, it is difficult to discuss the influence of the irrigation discharge and the timing of fertilization on the resulting uniformity. Nevertheless, it seems clear that A1 cases are not well suited for short fertilizer applications (with the exception of case A1Q3). The fertilizer plume infiltrates in a short fraction of the border and the resulting uniformity is very low. The A2 and A3 evaluations show the largest absolute fertilizer DULH, suggesting that in blocked end borders it is a good practice to start short fertilizer applications between 33% and 50% of advance. An increase in the irrigation discharge produces the same effect as increasing the fertilizer application time, since the mass of fertilizer is dissolved in a larger volume of water.

A linear regression between nitrate concentration ( $\text{mg l}^{-1}$ ) and EC ( $\text{dSm}^{-1}$ ) of the irrigation water was performed in order to assess the validity of the indirect measurement of nitrates. The resulting equation ( $\text{NO}_3^- = 514.7 \text{ EC} - 935.7$ ) was characterized by a high and significant determination coefficient ( $R^2 = 95.85\%$  ;  $P < 0.001$ ).

### **Assessing border fertigation performance**

**A1Q1 : Blocked-end border.** Fig. 7 presents a contour line map of fertilizer DULH corresponding to all possible combinations of  $t_s$  and  $t_e$ . Due to the high irrigation water DULH (96.3%), the best solution is to apply the fertilizer continuously with irrigation water. Short application times (located along the diagonal line) do not represent an adequate choice in this case, for they stand good chances of reaching the irrigation advance front where they will be infiltrated in a short time. Under these circumstances the fertilizer uniformity is low. It is interesting to note that short applications starting late in the irrigation event yield better

uniformities than applications started early. This is due to the field slope, which will transport the fertilizer downstream independently of how late it is applied.

**A1Q1-LB : Level Basin.** Eliminating the slope of case A1Q1 results in very different fertigation results. Fig. 8 indicates that uniform fertilizer applications must either start at  $t = 0$  min and end beyond 60 min, or start before 60 min and end at the time of cut-off. If a short application is to be made, the range of 40-60 min is the best suited, although the results will be poor ( $40\% < \text{DULH} < 50\%$ ). The mentioned range in times corresponds to a range of 33-50% of advance distance. The absence of slope determines the extremely low fertilizer DULH associated with short and late applications. Shortly after the fresh water reaches the downstream end of the basin, the fertilized water behind stagnates and infiltrates in place. In coincidence with case A1Q1, the best solution is to apply the fertilizer continuously with irrigation water.

**A1Q1-SRO : Free draining border with runoff fertilizer losses.** The analysis of this case study must be conducted by simultaneous study of Figs. 9 and 10. Fig. 9 offers two good options to obtain a good fertilizer uniformity : 1) apply fertilizer from the beginning of the irrigation event and finish as late as possible (beyond 50 min); and 2) make a short application starting at about 70 min. Unfortunately, the second option will release between 50 and 60% of the fertilizer to the runoff stream (Fig. 10). In this case, an appropriate solution could be an application between times 0 and 70 min (fertilizer DULH = 87% ; fertilizer runoff = 2.5%).

**A1Q1-DP : Deep percolation losses.** The parameters of the surface irrigation event yield an average water application of 216 mm. In most irrigated soils more than half of this water will be lost by deep percolation. Without further consideration of the interaction between the water, the solute and the soil porous medium, it seems like a good practice to apply the fertilizer late in the irrigation event, so that it has more chances to remain in the soil and not be washed out by deep percolation. Fig. 11 presents the corresponding contour line map of fertilizer DULH. The best uniformity is obtained for applications between 200 and 450 min. In this case the

fertilizer DULH reaches a value of 95.6%, larger than the water DULH (85.7%). In order to minimize deep percolation losses of fertilizer, it would be advisable to delay fertilizer application as much as possible. In this sense, it is interesting to note that even a late and short application such as between times 475 and 500 min has a fertilizer DULH (89.8%) larger than the water DULH. The chances for deep percolation losses of fertilizer will be much reduced in this case.

## **Conclusions**

The proposed fertigation evaluation technique (based on the combination of typical evaluation procedures and the time evolution of the fertilizer concentration in irrigation water) has yielded estimates of fertilizer application in agreement with soil measurements. Evaluation alone can be a very good tool to improve fertigation policies. In this sense, the complexity and expense of determining the fertilizer concentration can be avoided by using field EC meters. A regression line can be determined locally to estimate fertilizer concentration from water EC based on a few fertilizer determinations. If no regression line is available, the EC meter can be used in the field to establish the location of the fertilizing plume and improve the fertilizer application rules iteratively.

The simplified model of border fertigation was used to simulate the bromide and nitrate experiments. The correlation between measured and predicted application was very good in the bromide experiment, while in the nitrate experiment the model could only explain 29.3% of the estimated nitrate application and 43.8% of the fertilizer DULH. When compared with fertilizer uniformity estimations, model predictions are usually low. This is due to the neglect of differential convection and turbulent diffusion. The DULH estimated with the model can be considered as a lower bound of actual fertilizer uniformity. Our results also suggest that the spatial variability of infiltration could determine the advance of the plume of fertilized water and therefore the fertilizer uniformity.

According to field experiments and model predictions, when the fertilizer is applied in a short time interval the uniformity of surface fertigation is usually lower than the irrigation uniformity. If a point fertilizer application is to be made, the best uniformities will probably be obtained if the fertilizer is applied between 33 and 50 % of complete advance. When dealing with level-basin irrigation, late fertilizer applications must be avoided to prevent particularly poor uniformities.

The presented model can be applied to the determination of a fertilization policy specifically adapted to a given irrigation event. Procedures have been discussed to optimize fertilizer application in the presence of large runoff and deep percolation losses. In any case, reference has to be made to a continuous application of fertilizer from time 0 to time  $t_c$ . If the water uniformity and efficiency of the irrigation event are high, the latter will definitely be the best fertilizer management option. In other cases, long applications of fertilizer (lasting about  $t_c/2$ ), shifted towards the beginning or the end of the irrigation, have proven useful in preventing fertilizer losses and/or improving the fertilizer uniformity beyond that of water application.

Future research should focus on the construction of more physically correct models, exploring the dynamics of fertilizer in overland water and the soil porous medium. A compromise should be found between model completeness and execution time. In this way, accurate results could be found at a small expense of computational time. This is particularly important since a good fertilizer application policy will have to be found for each irrigation event in an iterative fashion, involving tens or hundreds of fertigation simulations.

## **Acknowledgments**

We are very grateful to the large crew of field assistants formed by the staff and students of the Soils and Irrigation Department and by students from the Polytechnic School of La Almunia (University of Zaragoza). It would have been impossible to run the field experiments without their help in sample collection and processing.



## References

- Cunge JA, Holly FM, Verwey A (1980) Practical aspects of computational river hydraulics. Pitman Publishing Limited, 420 pp
- Hanson B, Bowers W, Davidoff B, Kasapligil D, Carvajal A, Bendixen W (1995) Field performance of microirrigation systems. In: Microirrigation for a changing world: Conserving resources/Preserving the environment. Proc. Fifth Int'l. Microirrigation Congress, Orlando, Florida, pp 769-774
- Izadi B, King B, Westermann D, McCann I (1996) Modeling transport of bromide in furrow-irrigated field. *J Irrig and Drain Engrg, ASCE*, 122(2):90-96
- Jaynes DB, Rice RC, Hunsaker DJ (1992) Solute transport during chemigation of a level basin. *Trans ASAE*, 35(6):1809-1815
- Katopodes ND (1994) Hydrodynamics of surface irrigation: Vertical structure of the surge front. *Irrig Sci*, 15:101-111
- Merriam JL, Keller J (1978) Farm irrigation system evaluation: a guide for management. Utah State University. Logan, Utah, 271 pp
- Nieto KF, Frankenberger WT (1985) Single column ion chromatography: I. Analysis of inorganic anions in soils. *Soil Sci. Soc. Am. J.* 49:587-592
- Tabatabai MA, Dick WA (1983) Simultaneous determination of nitrate, chloride, sulfate, and phosphate in waters by ion chromatography. *J. Environ. Qual.* 12:209-213
- Threadgill ED (1985) Chemigation via sprinkler irrigation : current status and future development. *Applied Engrg in Agric* 1:16-23
- Threadhill ED, Eisenhauer DE, Young JR, Bar-Yosef B (1990) Chemigation. In : Hoffman GJ, Howell TA, Solomon KH (eds) Management of Farm Irrigation Systems. American Society of Agricultural Engineers, St. Joseph, Michigan , pp 747-780
- Viets FG, Humbert RP, Nelson CE (1967) Fertilizers in relation to irrigation practice. In : Hagan RM, Haise HR, Edminster TW (eds) Irrigation of Agricultural Lands. Agronomy (11). American Society of Agronomy, Madison, Wisconsin , pp 1009-1023

Walker WR (1989) Guidelines for designing and evaluating surface irrigation systems. FAO Irrigation and Drainage paper 45. Food and Agriculture Organization of the United Nations. Rome, Italy, 137 pp

Walker WR (1993) SIRMOD, Surface irrigation simulation software. Utah State University. Logan, Utah, USA, 27 pp

## Glossary

*The following symbols are used in this paper:*

$a$  = empirical infiltration exponent;

$A$  = solute application [ $M L^{-2}$ ];

$C$  = solute concentration of overland irrigation water [ $M L^{-3}$ ];

$DSBC$  = location of the downstream boundary condition [L];

$DULH$  = Distribution uniformity of the low half;

$DULQ$  = Distribution uniformity of the low quarter;

$f_0$  = empirical infiltration coefficient [ $M T^{-1}$ ];

$h$  = flow depth [L];

$I$  = mass of infiltrated fertilizer [M];

$k$  = empirical infiltration coefficient [ $L T^{-a}$ ];

$K_x$  = longitudinal mixing coefficient;

$m$  = total number of water samples;

$M$  = total overland mass of fertilizer [M];

$MF$  = total mass of applied fertilizer [M];

$n$  = Manning roughness coefficient;

$Q$  = Unit inflow discharge [ $L^2 T^{-1}$ ];

$SRO$  = mass of fertilizer lost by surface runoff [M];

$t$  = time [T];

$t_s$  = starting time of fertilizer application [T];

$t_e$  = ending time of fertilizer application [T];

$t_c$  = time of cut-off [T];

$v$  = flow velocity [ $L T^{-1}$ ];

$W$  = border width [L];

$x$  = distance down the border [L];

$XA$  = location of the advancing front of fertilizer [L];

$XR$  = location of the recession front of fertilizer [L];

$Z$  = infiltrated water depth [L];

$\tau$  = opportunity time [T]; and

$\Omega = \text{constant [M]}$ ;

## List of Tables

**Table 1.** Selected parameters of the nine nitrate experiments : Inflow discharge ( $Q$ ,  $\text{ls}^{-1} \text{m}^{-1}$ ) ; border width ( $W$ , m) ; time of cut-off ( $t_c$ , min) ; and starting and ending fertilizer application times ( $t_s$  and  $t_e$ , min).

**Table 2.** Local and spatially averaged Kostiakov-Lewis infiltration parameters and corresponding coefficients of determination for the bromide experiment.

**Table 3.** Results of the nine nitrate experiments : Spatially averaged Kostiakov-Lewis infiltration parameters  $a$ ,  $k$  ( $\text{m min}^{-a}$ ) and  $f_0$  ( $\text{m min}^{-1}$ ) ; and water and fertilizer DULH and DULQ (%).

Table 1

Experiment	Q (l s <sup>-1</sup> m <sup>-1</sup> )	W (m)	t <sub>c</sub> (min)	t <sub>s</sub> (min)	t <sub>e</sub> (min)
A1Q1	3.21	3.55	76	0	5
A1Q2	5.31	3.49	62	0	5
A1Q3	7.61	2.90	45	0	5
A2Q1	3.23	3.55	48	20	25
A2Q2	5.24	3.55	60	20	25
A2Q3	8.24	2.90	30	13	18
A3Q1	3.64	3.55	60	39	44
A3Q2	4.22	3.49	64	44	49
A3Q3	7.61	2.90	37	23	28

Table 2

Type	Distance (m)	k (m min <sup>-a</sup> )	a	f <sub>0</sub> (m min <sup>-1</sup> )	R <sup>2</sup> (%)
Local	25	0.007552	0.4027	0.0000	97.4
	75	0.013225	0.2895	0.0000	98.6
	125	0.005733	0.4515	0.0000	88.8
	175	0.002843	0.5904	0.0000	97.8
	225	0.008010	0.3953	0.0000	95.8
Spatially Averaged	-	0.006562	0.4347	0.0000	75.5

Table 3

Experiment t	k (m min <sup>-a</sup> )	a	f <sub>0</sub> (m min <sup>-1</sup> )	<u>Estimated Fertilizer</u>		<u>Predicted Fertilizer</u>		<u>Predicted Water</u>	
				DULQ (%)	DULH (%)	DULQ (%)	DULH (%)	DULQ (%)	DULH (%)
A1Q1	0.0187	0.166	0.00016	4.38	6.06	0.00	0.00	92.56	96.28
A1Q2	0.0270	0.166	0.00014	1.65	2.88	0.00	0.00	92.43	96.88
A1Q3	0.0234	0.166	0.00010	19.98	30.78	0.00	0.00	73.20	76.34
A2Q1	0.0080	0.166	0.00010	25.79	33.59	28.81	30.59	66.91	71.38
A2Q2	0.0240	0.174	0.00014	41.58	51.58	12.46	27.39	90.03	91.34
A2Q3	0.0065	0.166	0.00008	9.79	11.10	8.42	9.82	34.11	38.49
A3Q1	0.0180	0.166	0.00008	13.88	19.38	28.53	31.05	90.66	92.58
A3Q2	0.0300	0.174	0.00007	30.06	39.94	26.52	29.95	92.41	96.73
A3Q3	0.0130	0.166	0.00017	21.36	28.55	14.74	17.80	59.39	63.50

## List of Figures

**Figure 1.** Schematic representation of a surface fertigation event at times  $t$  and  $t+\Delta t$ .

**Figure 2.** Water advance-recession diagrams for the bromide field experiment. Symbols indicate observed values and solid lines present model predictions. The model predicted advance and recession trajectories of the plume are presented in dashed lines.

**Figure 3.** Water bromide concentration vs. opportunity time at different locations down the border. The plots present measured and model predicted concentrations.

**Figure 4.** Measured, estimated and predicted bromide application vs. distance down the border.

**Figure 5.** Estimated (symbols) and model predicted (lines) fertilizer application for the nine nitrate experiments. Experiment names express combinations of three fertilizer application timings (0, 33 and 50% of advance : A1, A2 and A3, respectively), and three inflow discharges (increasing from Q1 to Q3).

**Figure 6.** Estimated vs. model predicted nitrate DULH (%) for the nine nitrate experiments.

**Figure 7.** Contour line representation of fertilizer DULH (%) for experiment A1Q1 considering all possibilities of starting and ending times of fertilizer application.

**Figure 8.** Contour line representation of fertilizer DULH for experiment A1Q1-LB considering all possibilities of starting and ending times of fertilizer application.

**Figure 9.** Contour line representation of fertilizer DULH (%) for experiment A1Q1-SRO considering all possibilities of starting and ending times of fertilizer application.

**Figure 10.** Contour line representation of fertilizer runoff (%) for experiment A1Q1-SRO considering all possibilities of starting and ending times of fertilizer application.

**Figure 11.** Contour line representation of fertilizer DULH (%) for experiment A1Q1-DP considering all possibilities of starting and ending times of fertilizer application.

Figure 1

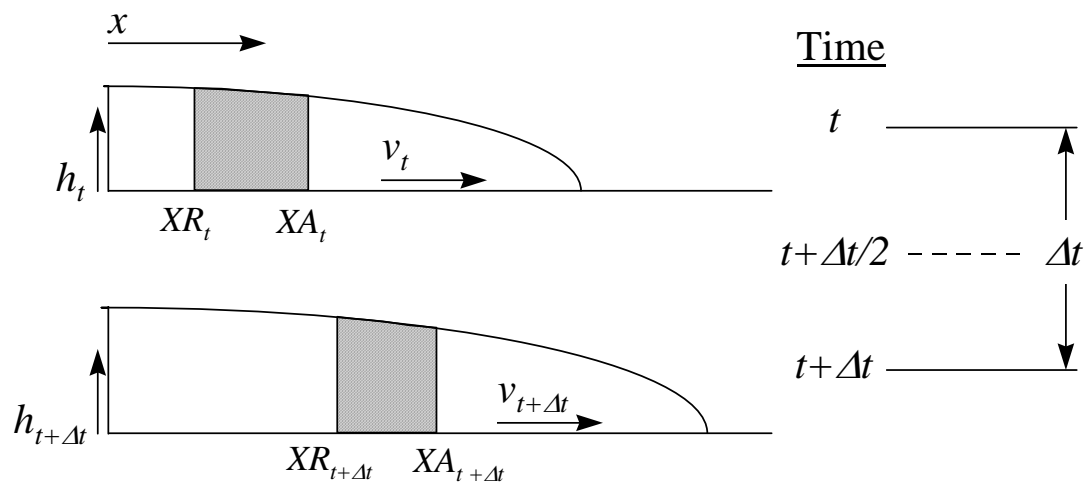


Figure 2

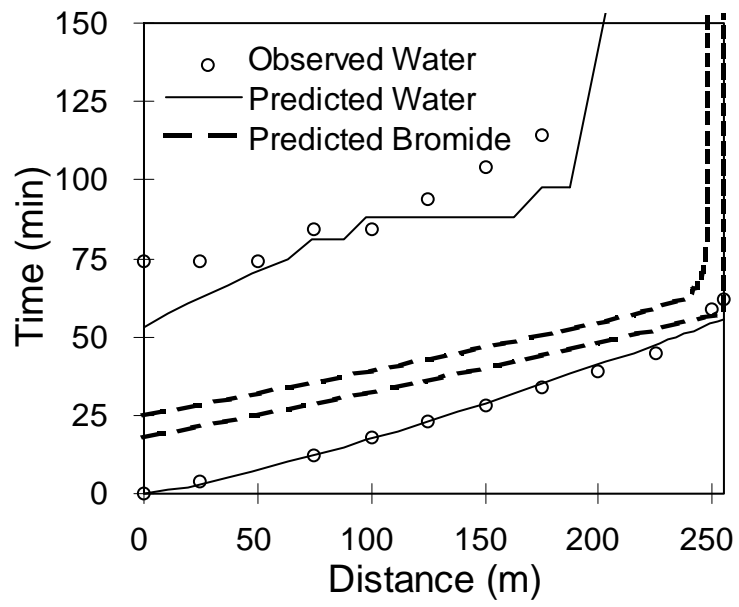


Figure 3

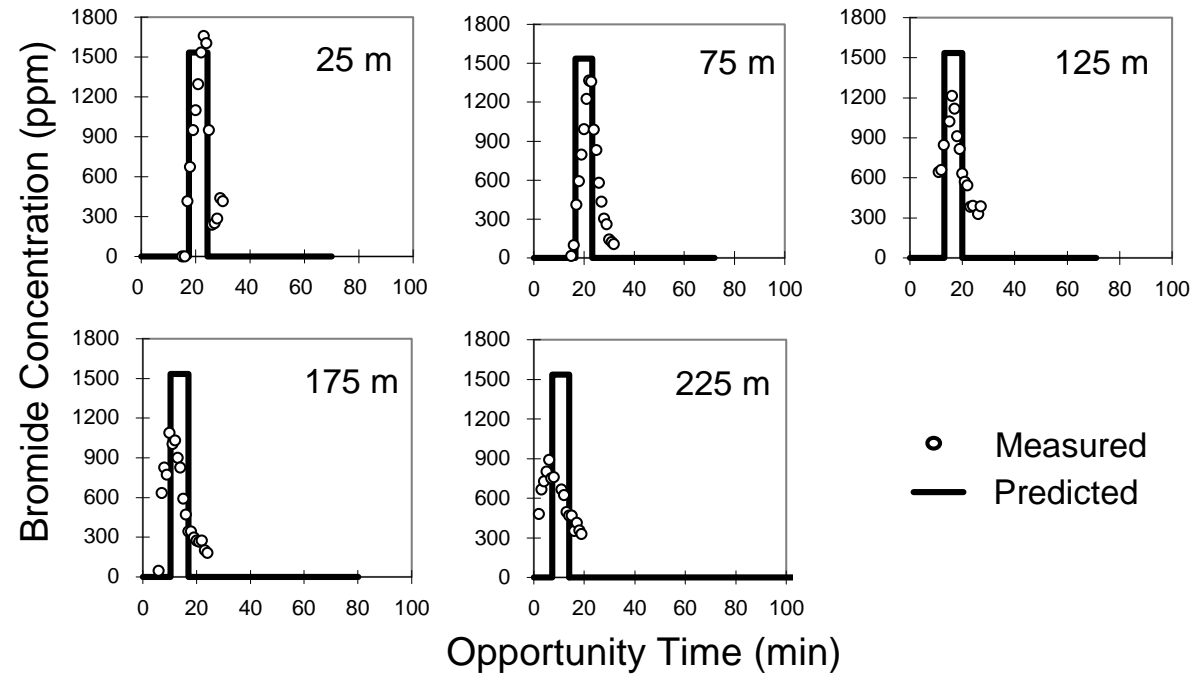


Figure 4

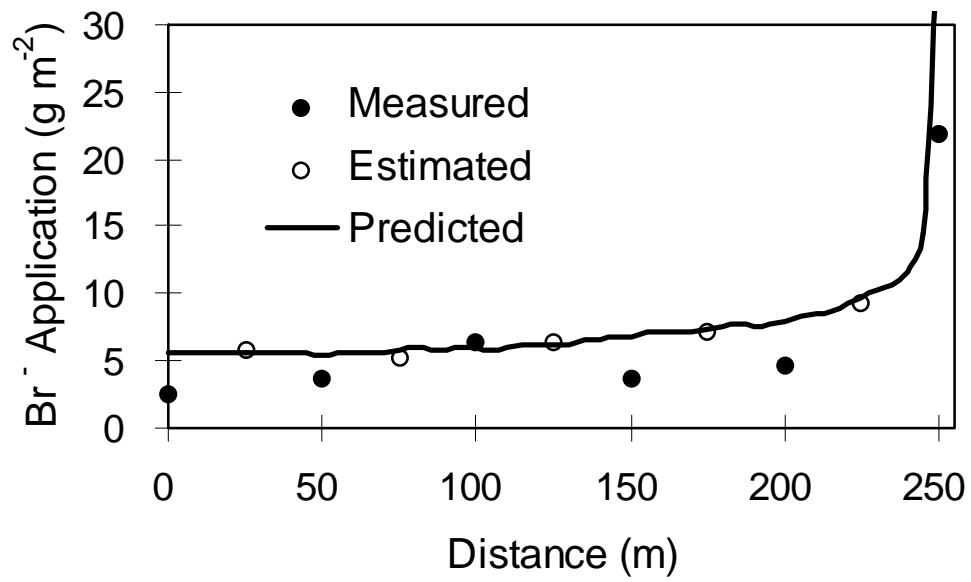


Figure 5

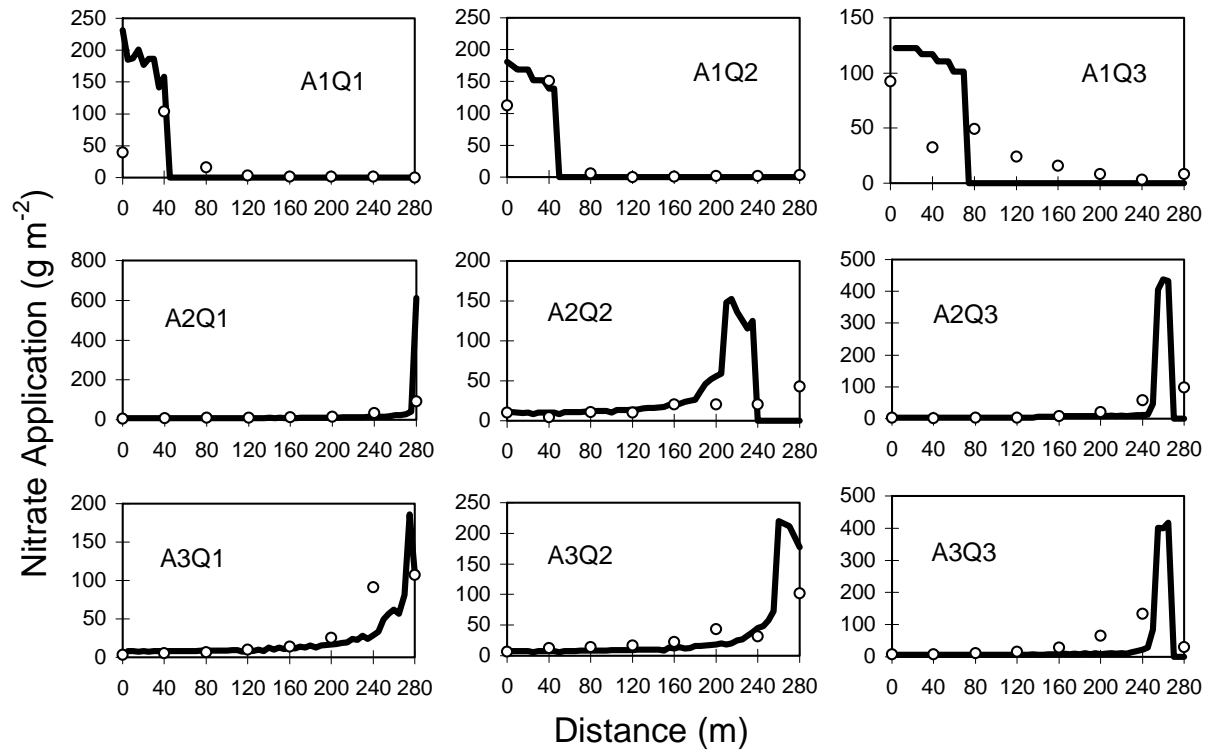


Figure 6

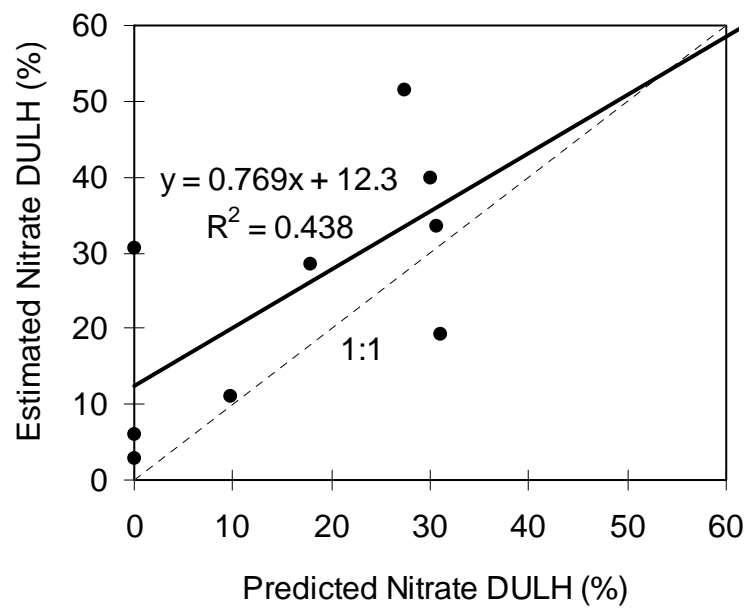


Figure 7

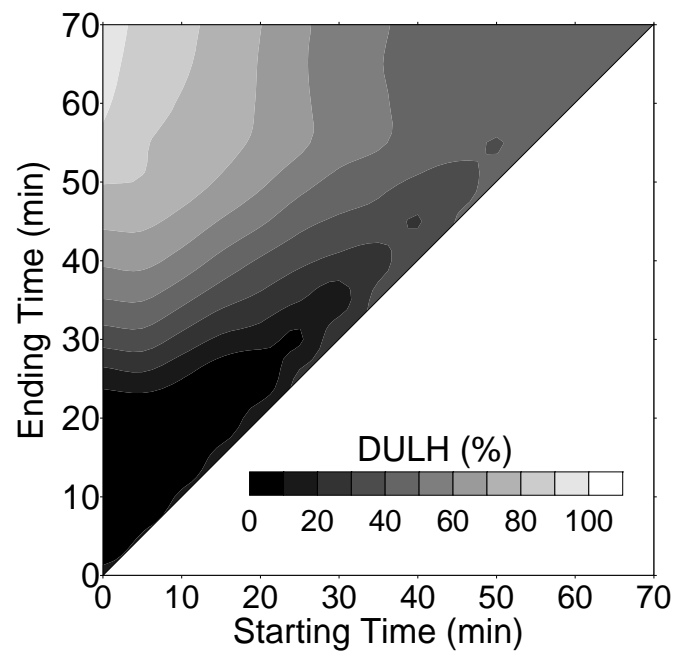


Figure 8

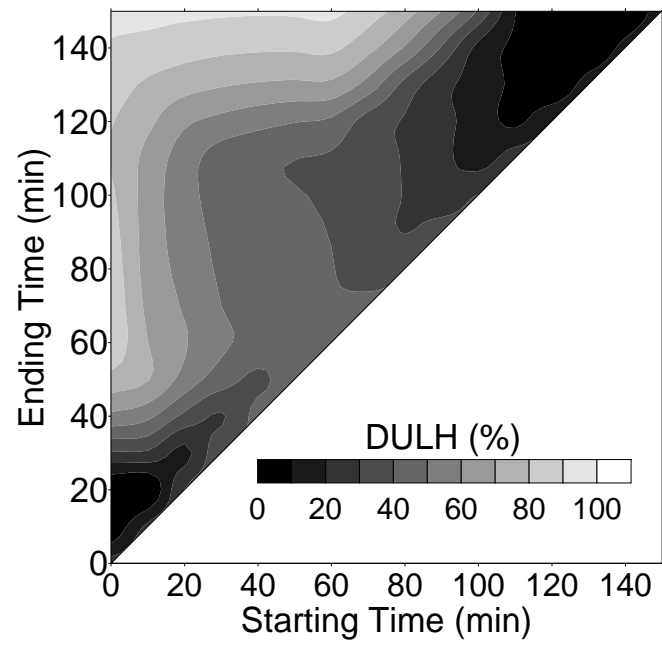


Figure 9

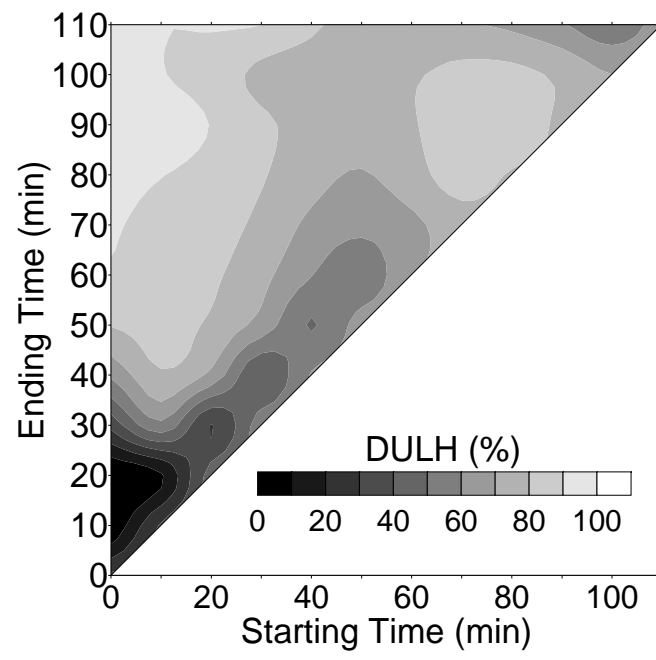


Figure 10

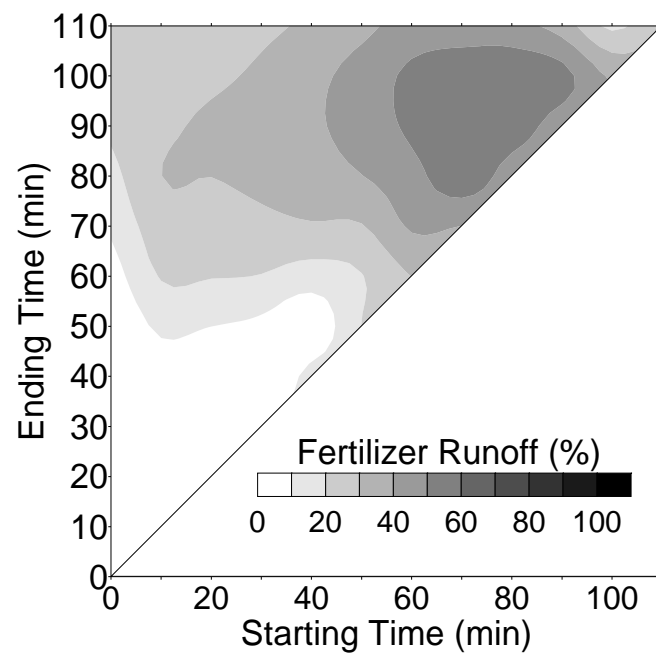


Figure 11

